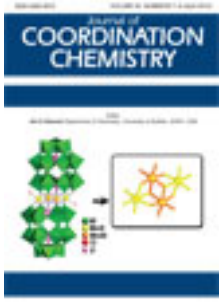


Journal of Coordination Chemistry
Publication details, including instructions for authors and subscription information:
http://www.tandfonline.com/loi/gcoo20

# Micellar catalysis on picolinic acid promoted hexavalent chromium oxidation of glycerol

Sumanta K. Ghosh [a], Ankita Basu [a], Rumpa Saha [a], Aniruddha Ghosh [a], Kakali Mukherjee [a] & Bidyut Saha [a]
[a] Department of Chemistry, The University of Burdwan, Burdwan - 713104, West Bengal, India
Published online: 13 Mar 2012.

To cite this article: Sumanta K. Ghosh, Ankita Basu, Rumpa Saha, Aniruddha Ghosh, Kakali Mukherjee & Bidyut Saha (2012) Micellar catalysis on picolinic acid promoted hexavalent chromium oxidation of glycerol, Journal of Coordination Chemistry, 65:7, 1158-1177, DOI: 10.1080/00958972.2012.669035

To link to this article: http://dx.doi.org/10.1080/00958972.2012.669035

*Journal of Coordination Chemistry*
Vol. 65, No. 7, 10 April 2012, 1158–1177



# Micellar catalysis on picolinic acid promoted hexavalent chromium oxidation of glycerol†

SUMANTA K. GHOSH, ANKITA BASU, RUMPA SAHA*, ANIRUDDHA GHOSH, KAKALI MUKHERJEE and BIDYUT SAHA*

Department of Chemistry, The University of Burdwan, Burdwan – 713104, West Bengal, India

(*Received 27 September 2011; in final form 2 January 2012*)

Under pseudo-first-order conditions, monomeric Cr(VI) was found to be kinetically active in the absence of picolinic acid (PA), whereas in the PA-promoted path, the Cr(VI)–PA complex undergoes nucleophilic attack by the substrate to form a ternary complex which subsequently experiences redox decomposition, leading to glyceraldehydes and Cr(IV)–PA complex. The uncatalyzed path shows a second-order dependence on $[H^+]$, whereas the PA-catalyzed path shows zero-order dependence on $[H^+]$. Both the uncatalyzed and PA-catalyzed path show a first-order dependence on $[glycerol]_T$ and $[Cr(VI)]_T$. The PA-catalyzed path is first order in $[PA]_T$. All these observations remain unaltered in the presence of externally added surfactants. The effect of the cationic surfactant cetyl pyridinium chloride (CPC) and anionic surfactant sodium dodecyl sulfate (SDS) on the PA-catalyzed path have been studied. CPC inhibits, whereas SDS accelerates the reaction. Here, SDS is a catalyst for glyceraldehydes production and at the same time reduction of carcinogenic hexavalent chromium to nontoxic trivalent chromium. The reaction proceeds simultaneously in both aqueous and micellar phase. Micellar effects have been explained by considering the preferential partitioning of reactants between the micellar and aqueous phase. The Menger–Portnoy model, Piszkiewicz cooperative model, and pseudo-phase ion exchange model have been tested to explain the observed micellar effect.

*Keywords*: Micellar catalysis; Oxidation; Chromium; Glycerol; Menger–Portnoy model; Piszkiewicz cooperative model; Pseudo-phase ion exchange



## 1. Introduction

Application and analysis of aggregation of surfactants is a hot topic [1]. The studies on the effect of organized assemblies on the conversion of reactant to product have received considerable attention [2]. The effect of organized assemblies on the rate of the reaction can be attributed [2, 3] to hydrophobic and electrostatic interaction in partition of the reactants. Aggregation of surfactants is known as micelle; micellar systems are well-studied for separation [4] and catalytic processes [5–7]. For catalytic processes, micellar solutions provide alternative synthetic routes to aqueous medium. In an

*Corresponding authors. Email: rumu.chem@gmail.com; b_saha31@rediffmail.com
†Dedicated to Sri Ramakrishna Param Padapadya.


ISSN 0095-8972 print/ISSN 1029-0389 online 
http://dx.doi.org/10.1080/00958972.2012.669035

aqueous phase, the surface active agents or surfactant molecules aggregate at ambient conditions forming micelles with hydrophobic cora and hydrophilic corona [6b]. Micellar catalysis has also received considerable attention with analogies drawn between micellar and enzyme catalysis [8–10]. Hexavalent chromium is a strong oxidant [11]. Here we report a method for glyceraldehydes production using micelles as catalysts, although it is not a feasible route from an economical point of view and at the same time the reduction of carcinogenic hexavalent chromium [11] to nontoxic trivalent chromium occurs. The purpose of this work is investigation into catalytic mechanisms. Picolinic acid (PA), bipyridine, and 1,10-phenanthroline are widely used as promoters for Cr(VI) oxidation of organic substrates [3, 12–16]. Recently, we reported bipy-promoted Cr(VI) oxidation of D-fructose [12], D-glucose [13], hexitols [14a], ethane-1,2-diol, and propan-2-ol [14b, c] in micellar media. It has been found [15, 16] that micelles significantly influence the kinetic and mechanistic aspects of Cr(VI) oxidation of different organic substrates, and the observed micellar effect can substantiate the proposed reaction mechanism. The applicability of different kinetic models, e.g., Menger–Portnoy model, Piszkiewicz cooperative model, and pseudo-phase ion exchange (PIE) model, has been tested to explain the observed micellar effect.



## 2. Experimental

### 2.1. *Materials and reagents*

Picolinic acid (PA) (m.p. 136°C) was recrystallized from MeOH. Glycerol (AR, Merck, India), $K_2Cr_2O_7$ (BDH, AR), sodium dodecyl sulfate (SDS) (AR, SRL, India), cetyl pyridinium chloride (CPC) (AR, SRL, India), $H_2SO_4$ (Merck, India), $HClO_4$ (Merck, India), and all other chemicals were of highest purity available commercially. Solutions were prepared by using doubly-distilled water.

### 2.2. *Procedure and kinetic measurements*

Solutions of the oxidant and reaction mixtures containing known quantities of substrate (S) (glycerol), catalyst (PA) {under the conditions $[S]_T \gg [Cr(VI)]_T$ and $[PA]_T \gg [Cr(VI)]_T$}, surfactant, acid, and other necessary chemicals were separately thermostated (±0.1°C). The reaction was initiated by adding the requisite amount of the oxidant with the reaction mixture. Progress of the reaction was monitored by following the decay of Cr(VI) at 415 nm at different time intervals with the UV-Vis spectrophotometer (UV 2401 PC, Shimadzu). Quartz cuvettes of path length 1 cm were used. The pseudo-first-order rate constants ($k_{obs}$, $s^{-1}$) were calculated from the slope of plots of $\ln(A_{415})$ *versus* time ($t$). Reproducible results giving first-order plots (correlation coefficient $r \geq 0.998$) were obtained for each reaction. A large excess (≥15 fold) of substrate was used in all kinetic runs. No interference due to other species at 415 nm was verified. Under the experimental conditions, the possibility of decomposition of surfactants by Cr(VI) was investigated and the rate of decomposition in this path was found to be kinetically negligible.

### 2.3. *Product analysis and stoichiometry*

The product analysis was carried out under the kinetic conditions: $[S]_T \gg [Cr(VI)]_T$. In a typical experiment, the substrate (0.25 mol), Cr(VI) (0.02 mol), and PA (0.06 mol) were dissolved in 1.0 mol dm$^{-3}$ $H_2SO_4$ (100 cm$^3$). The reaction mixture was allowed to stand in the dark for 24 h to ensure completion, as indicated by disappearance of the Cr(VI) color. Then the reaction mixture was treated overnight with an excess (*ca* 250 cm$^3$) of a saturated solution of 2,4-dinitrophenyl hydrazine (DNP) in 2 mol dm$^{-3}$ HCl. The precipitated 2,4-dinitrophenyl hydrazone was filtered off, dried, and recrystallized from EtOH. The hydrazone has a m.p. of 166–167°C, which conforms [17] to that of the hydrazone of glyceraldehydes.

The oxidation product of glycerol, i.e., glyceraldehydes, was also estimated gravimetrically as 2,4-dinitrophenyl hydrazone [18]. In the presence of PA, the same stoichiometry was also maintained. The experimentally observed ratio of $[Cr(VI)]_T/[glycerol]_T \approx 0.68$ (from three independent set of determinations). Thus, the overall stoichiometry of the reaction may be represented as

$$3CH_2(OH)CH(OH)CH_2(OH) + 2HCrO_4^- + 8H^+ \rightarrow 3CH_2(OH)CH(OH)CHO + 2Cr(III) + 8H_2O \quad (1)$$

The final fate of the Cr(III) species has been confirmed spectroscopically. The UV-Vis spectra (figures 1 and 2) were recorded (UV-Vis UV-2401 PC, Shimadzu).

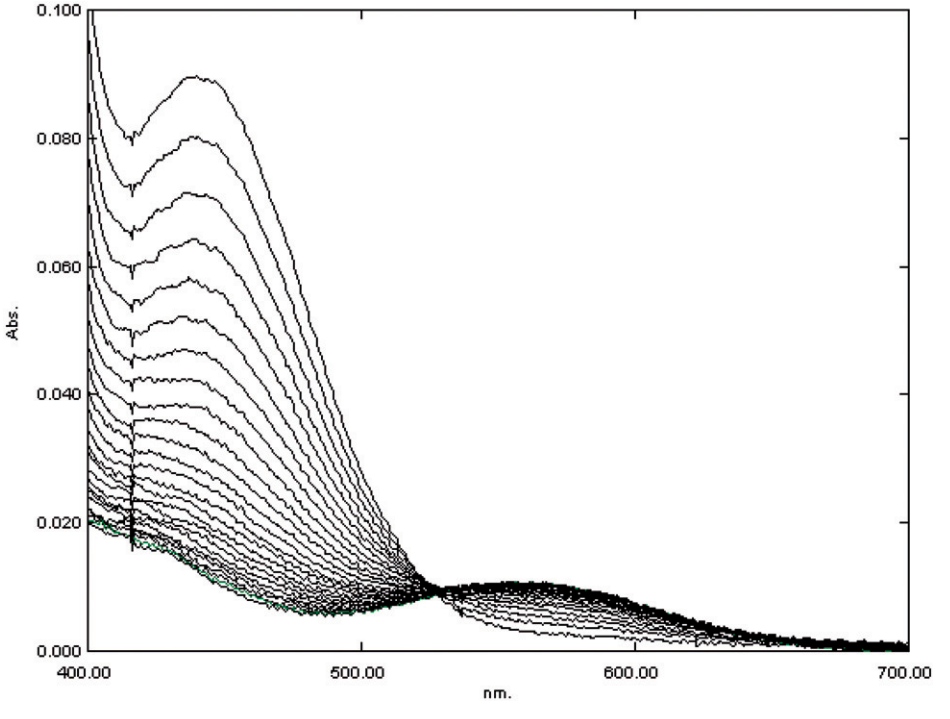


Figure 1. Absorption spectra of the reaction mixture at regular time intervals (5 min, e.g., at the beginning of the reaction, after 5 min, 10 min, etc. Concentrations at the beginning of the reaction: $[Cr(VI)]_T = 5.0 \times 10^{-4}$ mol dm$^{-3}$, $[PA]_T = 0.01$ mol dm$^{-3}$, $[H_2SO_4] = 0.5$ mol dm$^{-3}$, $[glycerol]_T = 0.05$ mol dm$^{-3}$, and $T = 30$°C.

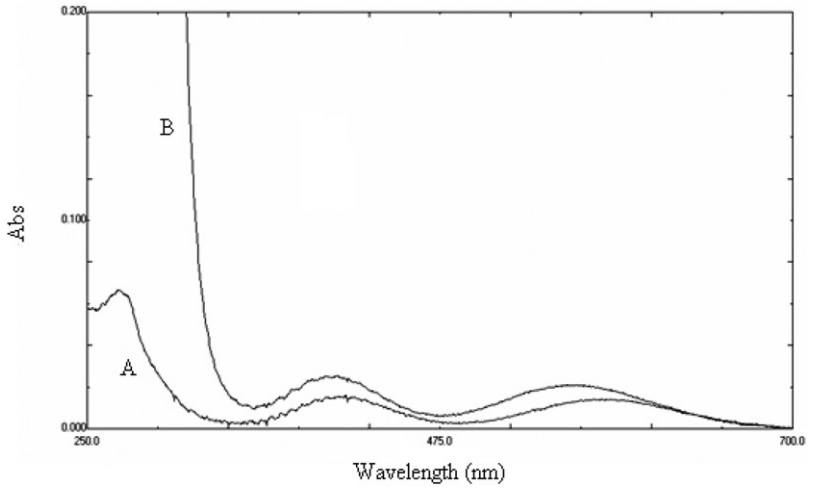


Figure 2. (A) Absorption spectrum of the reaction mixture (after completion of reaction): $[Cr(VI)]_T = 5 \times 10^{-4}$ mol dm$^{-3}$, $[glycerol]_T = 0.05$ mol dm$^{-3}$, $[PA]_T = 0$ mol dm$^{-3}$ (i.e., uncatalyzed path), and $[H_2SO_4] = 0.5$ mol dm$^{-3}$. (The spectrum of chromic sulfate is identical with this under the experimental condition.) (B) Absorption spectrum of the reaction mixture (after completion of reaction): $[Cr(VI)]_T = 5 \times 10^{-4}$ mol dm$^{-3}$, $[glycerol]_T = 0.05$ mol dm$^{-3}$, $[PA]_T = 0.01$ mol dm$^{-3}$, and $[H_2SO_4] = 0.5$ mol dm$^{-3}$.

The reaction solution was scanned (350–700 nm) at regular intervals to follow the gradual development of the reaction intermediate (if any) and the product. The scanned spectra (figure 1) indicate the gradual disappearance of Cr(VI)-species and appearance of Cr(III)-species with isosbestic point at $\lambda = 527$ nm. Observation of this single isosbestic point indicates very low concentration of probable intermediates like Cr(V) and Cr(IV) [19] under the present experimental conditions. In other words, it indicates the gradual decrease in Cr(VI) with the concomitant increase in Cr(III) concentration. The characteristic part of the electronic absorption spectrum of Cr(III)-species lies in the range 360–600 nm [20]. The color of the final solutions of the uncatalyzed and PA-catalyzed reactions are different due to the presence of different types of Cr(III)-species. The color of the final solution for the uncatalyzed reaction (i.e., in absence of PA) under the experimental condition is pale blue ($\lambda_{max} = 412$ and 578 nm) and the corresponding transitions [20] are 578 nm for $^4A_{2g}(F) \rightarrow {}^4T_{2g}(F)$ and 412 nm for $^4A_{2g}(F) \rightarrow {}^4T_{1g}(F)$ of the Cr(III)-species. On the other hand, the color of the final solution of the PA-catalyzed reaction under the identical condition is pale violet ($\lambda_{max} = 556$ nm for $^4A_{2g}(F) \rightarrow {}^4T_{1g}(F)$ of Cr(III) species). The spectra of the final solution of the uncatalyzed reaction and pure chromic sulfate solution in aqueous sulfuric acid media are identical, indicating that the final Cr(III)-species is simply Cr(III)-aqua species for the uncatalyzed reaction, whereas for the PA-catalyzed reaction, the final Cr(III) species is Cr(III)–PA complex. Similar results have been noted by earlier workers [21]. In the final solution of the PA-catalyzed reaction, there is a blue shift (figure 2) of the peak due to the transition $^4A_{2g}(F) \rightarrow {}^4T_{2g}(F)$ compared to the final solution of the uncatalyzed path. This blue shift is due to the presence of the strong donor (i.e., heteroatomic N-donor site of PA). For the Cr(III)–PA complex [31c], the peak due to the transition $^4A_{2g}(F) \rightarrow {}^4T_{1g}(F)$ merges with a charge transfer band (figure 2). For Cr(III)-aqua species, there is also a large charge transfer band [20] at

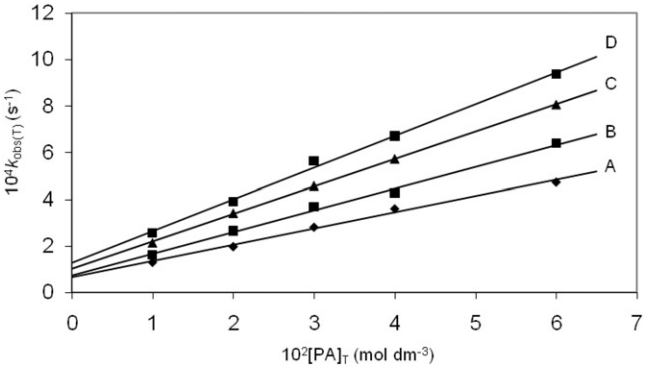


Figure 3. Dependence of $k_{obs(T)}$ on $[PA]_T$ for Cr(VI) oxidation of glycerol in aqueous $H_2SO_4$. $[glycerol]_T = 0.01\,mol\,dm^{-3}$, $[Cr(VI)]_T = 5 \times 10^{-4}\,mol\,dm^{-3}$, $[H_2SO_4] = 0.5\,mol\,dm^{-3}$, A (30°C), B (35°C), C (40°C), D (45°C).

higher energy. In fact, the band at 270 nm due to the $^4A_{2g}(F) \rightarrow {}^4T_{1g}(P)$ transition appears as a shoulder on the high-energy charge transfer band [20a]. The appearance of the charge transfer band at much lower energy for the proposed Cr(III)–PA complex is quite reasonable because of the favored metal-to-ligand charge transfer (MLCT). In fact, the vacant $\pi^*$ of PA favors MLCT. The existence of the charge transfer band (metal-to-ligand) at this lower energy for the PA-catalyzed reaction indirectly supports the presence of the Cr(III)–PA complex in the final solution.

## 3. Results and discussion

### 3.1. *Rate dependence on $[Cr(VI)]_T$*

Under the experimental condition $[S]_T \gg [PA]_T \gg [Cr(VI)]_T$, both in the presence and absence of PA, the rate of disappearance of Cr(VI) shows a first-order dependence on [Cr(VI)]. This first-order dependence is also maintained in the presence of the surfactants CPC, SDS, and TX-100. The pseudo-first-order rate constant ($k_{obs}$) has been evaluated from the linear plot of −log(absorbance of Cr(VI)) *versus* time (in min).

### 3.2. *Rate dependence on $[PA]_T$*

Plots of $k_{obs(T)}$ *versus* $[PA]_T$ are linear with positive intercepts measuring the contribution of relatively slower uncatalyzed path (figure 3). The pseudo-first-order rate constant $k_{obs(u)}$ directly measured in the absence of PA under the same conditions agrees with those obtained from the intercepts of the plots of $k_{obs(T)}$ *versus* $[PA]_T$. The observation is formulated as

$$k_{obs(T)} = k_{obs(u)} + k_{obs(c)} = k_{obs(u)} + k_{cat}[PA]_T \quad (2)$$

Both in the presence and absence of surfactants (CPC, SDS), the above relationship is valid. The values of $k_{cat}$ are given in table 1. During the progress of the reaction, PA is

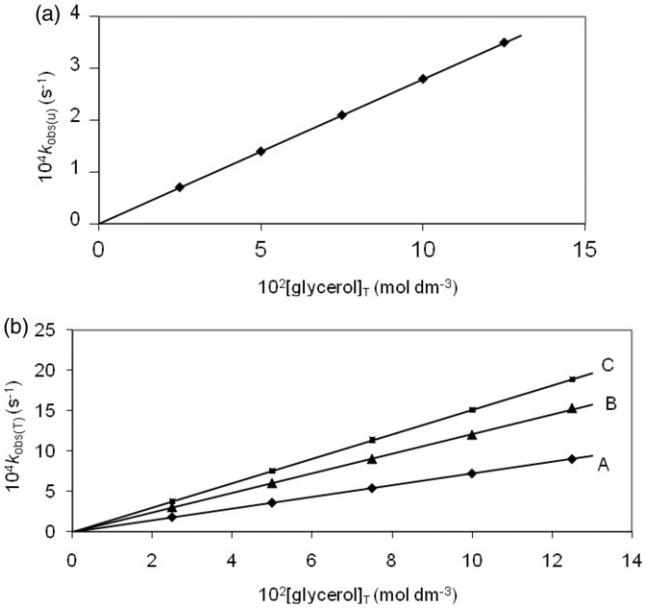


Figure 4. (a) Dependence of $k_{obs(u)}$ on $[glycerol]_T$ for Cr(VI) oxidation of glycerol in the absence of PA in aqueous $H_2SO_4$ at 30°C. $[Cr(VI)]_T = 5 \times 10^{-4}$ mol $dm^{-3}$, $[H_2SO_4] = 0.5$ mol $dm^{-3}$. (b) Dependence of $k_{obs(T)}$ on $[glycerol]_T$ for Cr(VI) oxidation of glycerol in presence of PA in aqueous $H_2SO_4$ at 30°C. $[Cr(VI)]_T = 5 \times 10^{-4}$ mol $dm^{-3}$, $[H_2SO_4] = 0.5$ mol $dm^{-3}$. $[PA] = 0.01$ mol $dm^{-3}$. A ($[CPC]_T = 2 \times 10^{-3}$ mol $dm^{-3}$; $[SDS]_T = 0$ mol $dm^{-3}$). B ($[CPC]_T = 0$ mol $dm^{-3}$; $[SDS]_T = 0$ mol $dm^{-3}$). C ($[CPC]_T = 0$ mol $dm^{-3}$; $[SDS]_T = 2 \times 10^{-2}$ mol $dm^{-3}$).

gradually lost due to the formation of the inert Cr(III)–PA complex. Under the experimental conditions, $[PA]_T \gg [Cr(VI)]_T$, it is reasonable to assume that $[PA]_T$ remains more or less constant.

### 3.3. *Rate dependence on $[S]_T$, i.e., $[glycerol]_T$*

The pseudo-first-order rate constant shows a first-order dependence on $[glycerol]_T$, both in the absence (figure 4a) and presence (figure 4b) of $[PA]_T$. Thus the relationship is

$$k_{obs(T)} = k_{s(T)}[S]_T = k_{s(c)}[S]_T + k_{obs(u)} \quad (3)$$

$$k_{obs(u)} = k_{s(u)}[S]_T \quad (4)$$

where $k_{s(c)}$ and $k_{s(u)}$ denote the corresponding PA-catalyzed and uncatalyzed path, respectively. This dependence pattern is also maintained in the presence of surfactant (such as SDS, CPC). The values of $k_{s(c)}$ are given in table 1.

### 3.4. *Rate dependence of $[H^+]$*

The acid dependence of $k_{obs}$ was studied in aqueous $HClO_4$ media, both in the presence and absence of PA. The acid concentration dependence patterns for the uncatalyzed and catalyzed paths are different. From the experimental fit (figure 5a and b), the

Table 1. Kinetic parameters and some representative rate constants for Cr(VI) oxidation of glycerol in the presence and absence of PA under different conditions, $[Cr(VI)]_T = 5 \times 10^{-4}$ mol dm$^{-3}$, $[H_2SO_4] = 0.5$ mol dm$^{-3}$.

| Temperature (°C) | $10^4 k_{obs(u)(w)}$ ($S^{-1}$)[a] | $10^3 k_{cat(w)}$ ($mol^{-1}\,dm^3\,S^{-1}$)[a] | $10^3 k_{cat(CPC)}$ ($mol^{-1}\,dm^3\,S^{-1}$)[b] | $10^3 k_{cat(SDS)}$ ($mol^{-1}\,dm^3\,S^{-1}$)[c] | $K_{eff(w)}$[d] | $10^3 k_{S(u)(w)}$ ($dm^3\,mol^{-1}\,S^{-1}$)[e] | $10^3 k_{s(c)(w)}$ ($dm^3\,mol^{-1}\,S^{-1}$)[f] | $10^3 k_{(c)\ (CPC)}$ ($dm^3\,mol^{-1}\,S^{-1}$)[g] | $10^3 k_{s(c)(SDS)}$ ($dm^3\,mol^{-1}\,S^{-1}$)[h] |
|---|---|---|---|---|---|---|---|---|---|
| 30 | 0.64 | 7.022 | 5.529 | 20.1 | 6.4 | 2.8 | 12.11 | 7.23 | 15.13 |
| 35 | 0.73 | 9.348 | | | 7.75 | | | | |
| 40 | 1.01 | 11.782 | | | 6.98 | | | | |
| 45 | 1.29 | 13.612 | | | 6.27 | | | | |
| $\Delta H^{\neq}$ (kJ $mol^{-1}$) | | 31.516 | | | | | | | |
| $\Delta S^{\neq}$ ($JK^{-1}\,mol^{-1}$) | | 181.95 | | | | | | | |

Subscript (u) for uncatalyzed, (c) for PA catalyzed path, (w) for the value in the absence of surfactant, (CPC) or (SDS) for the value in presence of the respective surfactant.
[a]$[Cr(VI)]_T = 5 \times 10^{-4}$ mol dm$^{-3}$, $[H_2SO_4] = 0.5$ mol dm$^{-3}$, $[S]_T = 0.01$ mol dm$^{-3}$, $[PA]_T = 0$–$0.06$ mol dm$^{-3}$.
[b]Conditions as in (a) and $[CPC] = 2 \times 10^{-3}$ mol dm$^{-3}$.
[c]Conditions as in (a) and $[SDS] = 2 \times 10^{-2}$ mol dm$^{-3}$.
[d]Conditions as in (a) and $k_{eff} = \{k_{obs(T)} - k_{obs(u)}\}/k_{obs(u)}$ and $k_{eff}$ calculated at $[PA]_T = 0.06$ mol dm$^{-3}$.
[e]$[Cr(VI)]_T = 5 \times 10^{-4}$ mol dm$^{-3}$, $[H_2SO_4] = 0.5$ mol dm$^{-3}$, $[S]_T = 0.025$–$0.125$ mol dm$^{-3}$.
[f]$[Cr(VI)]_T = 5 \times 10^{-4}$ mol dm$^{-3}$, $[H_2SO_4] = 0.5$ mol dm$^{-3}$, $[S]_T = 0.025$–$0.125$ mol dm$^{-3}$, $[PA]_T = 0.01$ mol dm$^{-3}$.
[g]$[Cr(VI)]_T = 5 \times 10^{-4}$ mol dm$^{-3}$, $[H_2SO_4] = 0.5$ mol dm$^{-3}$, $[S]_T = 0.025$–$0.125$ mol dm$^{-3}$, $[PA]_T = 0.01$ mol dm$^{-3}$, $[CPC] = 2 \times 10^{-3}$ mol dm$^{-3}$.
[h]$[Cr(VI)]_T = 5 \times 10^{-4}$ mol dm$^{-3}$, $[H_2SO_4] = 0.5$ mol dm$^{-3}$, $[S]_T = 0.025$–$0.125$ mol dm$^{-3}$, $[PA]_T = 0.01$ mol dm$^{-3}$, $[SDS] = 2 \times 10^{-2}$ mol dm$^{-3}$.

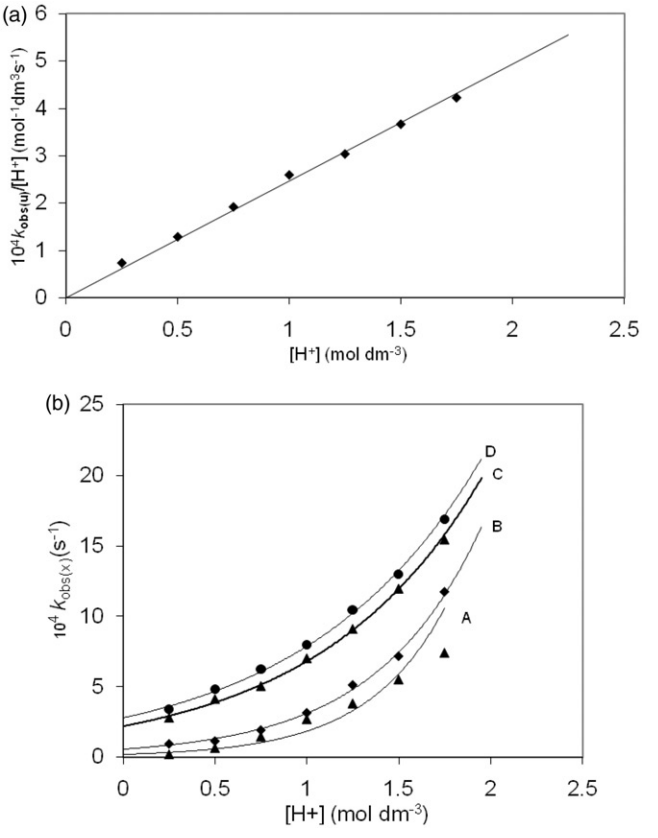


Figure 5. (a) Plot of $k_{obs(u)}/[H^+]$ *vs.* $[HClO_4]_T$. $[Cr(VI)]_T = 5 \times 10^{-4}$ mol dm$^{-3}$, $[glycerol]_T = 0.01$ mol dm$^{-3}$, $I = [HClO_4] + [NaClO_4] = 1.75$ mol dm$^{-3}$ (30°C). (b) Dependence of $k_{obs}$ on $[HClO_4]_T$ for Cr(VI) oxidation of glycerol in the presence of (i.e., $k_{obs(T)}$ for C and D) and absence of (i.e., $k_{obs(u)}$ for A and B) of PA in aqueous $HClO_4$ at 30°C. $[Cr(VI)]_T = 5 \times 10^{-4}$ mol dm$^{-3}$, $[glycerol] = 0.01$ mol dm$^{-3}$, $I = [HClO_4] + [NaClO_4] = 1.75$ mol dm$^{-3}$. A ($[PA]_T = [SDS]_T = 0$ mol dm$^{-3}$); B ($[PA]_T = 0$ mol dm$^{-3}$, $[SDS]_T = 2 \times 10^{-2}$ mol dm$^{-3}$); C ($[PA]_T = 0.02$ mol dm$^{-3}$, $[SDS]_T = 0$ mol dm$^{-3}$); D ($[PA]_T = 0.02$ mol dm$^{-3}$, $[SDS]_T = 2 \times 10^{-2}$ mol dm$^{-3}$).

observations are

$$k_{obs(u)} = k_{H(u)}[H^+]^2 \tag{5}$$

$$k_{obs(c)} = k_{obs(T)} - k_{obs(u)} = k_{H(c)}[H^+]^0 \tag{6}$$

A similar dependence pattern is also observed in the presence of SDS with enhanced rate constants.

### 3.5. *Test for acrylonitrile polymerization*

Under the experimental conditions, in the presence of PA, acrylonitrile was added under a $N_2$ atmosphere. On standing, polymerization starts indicating the formation of free radical intermediates in the reaction.

### 3.6. *Effect of temperature*

The effect of temperature on the catalytic path has been investigated in the 30–45°C range. Activation parameters ($\Delta H^{\neq}, \Delta S^{\neq}$) have been evaluated and are given in table 1.

### 3.7. *Mechanism of the reaction and rate law*

Product analysis indicates that glyceraldehydes are the main oxidation product, i.e., oxidation of the single primary hydroxyl group occurs. It has been noted [22] that in chromic acid oxidation of glycol containing $\alpha$-hydrogen, the energetically favorable reaction path leads to hydroxyaldehyde. Thus, the mechanism of the reaction can be divided into two sections: (i) uncatalyzed path and (ii) catalyzed path. Uncatalyzed path (scheme 1) for glycerol has been reported [23] earlier.

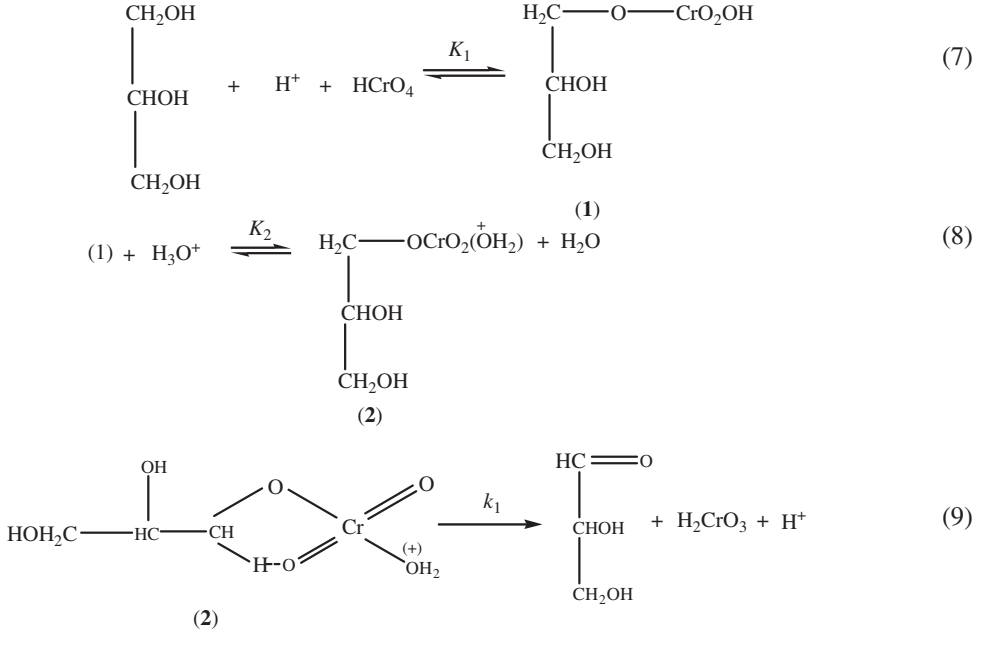


Scheme 1. Cr(VI) oxidation of glycerol in he absence of PA.

In the cyclic transition state **2**, reduction of Cr(VI) to Cr(IV) occurs [24] either through $H^+$ or $H^-$ transfer. In the next step, Cr(IV) is further reduced to Cr(III) by different possible routes [25, 26] as discussed below.

In the above routes, S (i.e., glycerol) is a 2e-reductant and $S^{\bullet}$ (i.e., $HOCH_2CH(OH)C^{\bullet}H(OH)$) is the partially oxidized product and P (product). In the Watanable–Westheimer mechanism [27] (i.e., Route 1) and Perez–Benito mechanism [26] (Route 3), the organic substrate behaves as a two-equivalent reductant throughout the reaction sequence, but in the Rocek mechanism [25] (i.e., Route 2), the organic substrate acts as a one-electron reductant toward Cr(IV) and as a two-electron reductant toward both Cr(VI) and Cr(V). In this mechanism Cr(IV) reacts with $HOCH_2CH(OH)CH_2(OH)$ to form Cr(III) and the free radical $HOCH_2$

$CH(OH)C^{\bullet}H(OH)$, which initiates polymerization of acrylonitrile, and this radical isultimately oxidized to $HOCH_2CH(OH)CHO$ by Cr(VI). The Rocek mechanism has been widely accepted for the Cr(VI) oxidation of many organic compounds, but Bontchev *et al*. [28] have supported the Watanable–Westheimer mechanism for Cr(VI) oxidation of various organic substrates. Previously, the route involving Cr(II) (i.e., the Perez–Benito mechanism) was dismissed because of the instability of Cr(II), but in the recent past, it has been established [25] that this mechanism really operates for different organic compounds including alcoholic substances. In fact, Cr(IV) is reduced to Cr(II) through a hydride transfer (i.e., 2e transfer) mechanism from the C–H bond of the $CH_2$–OH moiety. The hydride ion transfer during reduction of Cr(IV) generates an intermediate carbocation center, which is responsible for acrylonitrile polymerization [29].

$$\text{Route 1 :}\quad \text{Cr(IV)} \xrightarrow{\text{Cr(VI)}} 2\text{Cr(V)} \xrightarrow{2\text{S}} 2\text{Cr(III)} + 2\text{P} \qquad (10)$$

$$\text{Route 2 :}\quad \text{Cr(IV)} \xrightarrow{\text{S}} \text{Cr(III)} + \text{S}^{\cdot} \qquad (11)$$

$$\text{Cr(VI)} \xrightarrow{\text{S}^{\cdot}} \text{Cr(V)} \xrightarrow{\text{S}} \text{Cr(III)} + \text{P} \qquad (12)$$

$$\text{Route 3 :}\quad \text{Cr(IV)} \xrightarrow{\text{S}} \text{Cr(II)} + \text{P} \xrightarrow{\text{Cr(VI)}} \text{Cr(III)} + \text{Cr(V)} \qquad (13)$$

$$\text{Cr(V)} \xrightarrow{\text{S}} \text{Cr(III)} + \text{P} \qquad (14)$$

In scheme 1, the equilibrium constants $K_1$ and $K_2$ are expected to be quite low and lead to the following rate law:

$$\begin{aligned} k_{\text{obs(u)}} &= (2/3)K_1K_2k_1[\text{S}]_{\text{T}}[\text{H}^+]^2 \\ &= k_{\text{u}}[\text{S}]_{\text{T}}[\text{H}^+]^2 \\ &= k_{\text{s(u)}}[\text{S}]_{\text{T}} = k_{\text{H(u)}}[\text{H}^+]^2 \end{aligned} \qquad (15)$$

Here it is important to note that the intermediate ester could not be characterized and no kinetic evidence for its formation was available. However, such an ester formation mechanism is well-documented [30] for substrate having –OH groups.

For the PA-catalyzed path, scheme 2 can explain all the experimental findings. In this path, the formation of the Cr(III)–PA complex characterized spetroscopically indicates complexation of PA with the higher oxidation states of chromium (which are labile). Due to the inertness of Cr(III) ($t_{2g}^3$), the ligand does not enter into the inner coordination sphere of Cr(III) produced after the reduction of Cr(VI). Based on this argument, it is reasonable to consider that the Cr(VI)–PA complex (**4**) formed in the pre-equilibrium step (equation (17)) is an active oxidant [31]. Under the experimental conditions, the first-order dependence on $[\text{PA}]_{\text{T}}$ is strictly maintained throughout the range of $[\text{PA}]_{\text{T}}$ used, but it is worth mentioning that the increase in rate with increasing concentration of $[\text{PA}]_{\text{T}}$ restricts within a certain range of $[\text{PA}]_{\text{T}}$. Hence, it is reasonable to conclude that the equilibrium constant ($K_3$) for the reaction leading to cyclic Cr(VI)–PA complex (**4**) is very low. This is why, there is no kinetic evidence in favor of the formation of **4**. There is also no spectroscopic evidence for the suggested complex, i.e.,

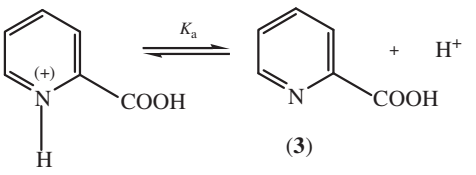


(3) (16)

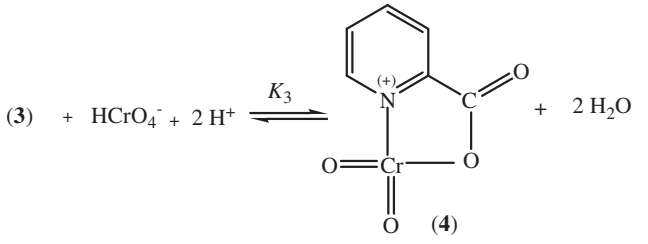


(17)

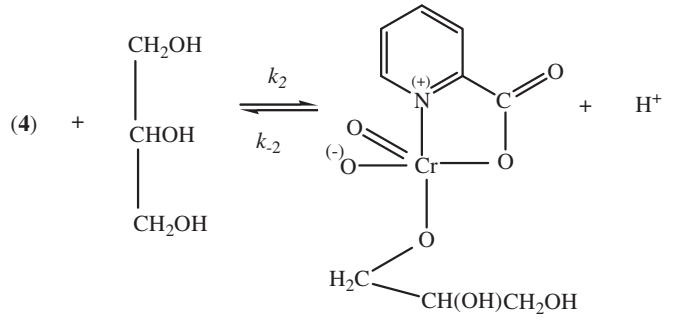


(5) (18)

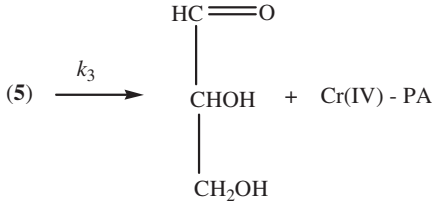


(19)

Scheme 2. PA catalyzed Cr(VI) oxidation of glycerol.

the spectrum of chromic acid does not change on addition of PA. The absence of spectroscopic evidence under the experimental conditions is due to the very low value of equilibrium constant for the formation of the complex. However, the absence of kinetic and spectroscopic evidence does not necessarily rule out the formation of the suggested complex.

In the next step, the Cr(VI)–PA complex reacts with the substrate to form ternary complex (**5**) which undergoes a redox decomposition (through hydrogen ion or hydride ion) transfer [24] in a rate-limiting step, giving rise to the organic product and the Cr(IV)–PA complex which may participate in subsequent faster steps as mentioned for

the uncatalyzed path. Scheme 2 leads to the following rate equation under steady-state conditions of the suggested ternary complex (**5**).

$$k_{obs(c)} = (2/3)(K_a K_3 k_2 k_3 [PA]_T [S]_T [H^+]^2 / \{(k_{-2}[H^+] + k_3)([H^+] + K_a)\} \quad (20)$$

Neglecting $K_a$ ($=0.025\,mol\,dm^{-3}$ at 25°C) [32] compared to $[H^+] = 0.25$–$1.75\,mol\,dm^{-3}$, and considering $k_{-2}[H^+] \gg k_3$, equation (20) reduces to equation (21), which explains the zero-order dependence on hydrogen ions. Here, it is interesting to note that the proposed ternary complex (**5**) remains in a reversible equilibrium, i.e., the $k_{-2}$ path (acid catalyzed) is much faster than the $k_{-3}$ path (acid-independent). Such an observation has been noted in earlier investigations with substrates such as methanol [31a], formic acid [31b], maleic acid [31c], lactic acid [31d], malic acid [31d], L-sorbose [31e], and hexitols [31f].

$$k_{obs(c)} = (2/3)(K_a K_3 k_2 k_3 [PA]_T [S]_T [H^+])/k_-2[H^+] = k_{cat}[PA]_T = k_{S(c)}[S]_T \quad (21)$$

Equation (21) conforms to the experimentally observed rate equation. The catalytic efficiency ($k_{eff}$) defined by $k_{eff} = \{k_{obs(T)} - k_{obs(u)}\}/k_{obs(u)}$ at $[PA]_T = 0.06\,mol\,dm^{-3}$ is of the order of 6–8 (cf table 1). The catalytic efficiency of PA probably arises from enhancement of the reduction potential of the Cr(VI)/Cr(IV) and Cr(VI)/Cr(III) couples through the stabilization of Cr(VI) and Cr(III), respectively, in the presence of PA. The entropy of activation $\Delta S^{\neq}$ for $k_{cat}$ is highly negative, in agreement with the proposed cyclic transition state.

The reactions are inhibited by CPC and catalyzed by SDS (figures 6 and 7; table 1). The rate constants under different conditions are given in table 1. To represent the rate constant in the presence of surfactants, the subscripts CPC and SDS have been used, while for the values in the absence of surfactants, the subscript w is used.

### 3.8. *Effect of surfactants*

Figures 6 and 7 show that the cationic surfactant CPC retards the rate of the reaction, while the anionic surfactant SDS accelerates the rate of the reaction.

**3.8.1. Effect of CPC.** CPC, a representative cationic surfactant, retards both the uncatalyzed and catalyzed paths. The plot of $k_{obs}$ *versus* $[CPC]_T$ (figure 6) shows a continuous decrease, and finally tends to level off at higher concentrations of CPC. This observation is similar to that observed by Bunton and Cerichelli [33] in the oxidation of ferrocene by Fe(III) salts in the presence of cationic cetyl trimethyl ammonium bromide. Similar observations have also been noted by Panigrahi and Sahu [34] in the oxidation of acetophenone by Ce(IV) and by Sarada and Reddy [35] in the oxalic acid catalyzed oxidation of aromatic azo compounds by Cr(VI) in the presence of SDS. The neutral triol is likely preferably partitioned in the micellar phase and the kinetically active $H_2CrO_4$ species [36] may remain concentrated in the stern layer of the micellar phase [37]. This leads to generation of the Cr(VI)-triol ester (**1**) in the micellar interphase. Thus, in the uncatalyzed path, the neutral Cr(VI)-substrate ester (**1**) formed (equation (7)) is partitioned in the micellar pseudo-phase of the surfactant, but the cationic surfactant repelling $H^+$ needed for the reaction (equation (8)) retards the reaction. In the PA-catalyzed path, CPC restricts the positively charged Cr(VI)–PA

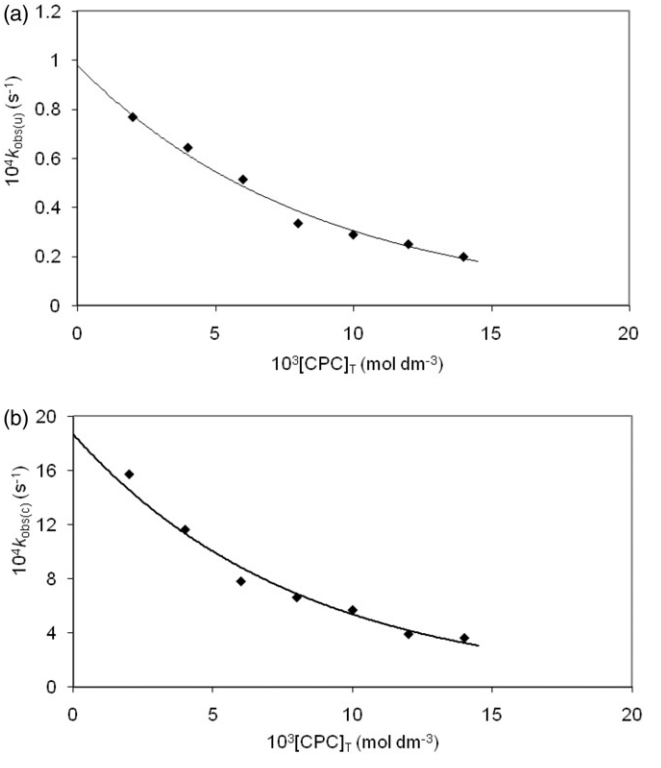


Figure 6. (a) Dependence of $[CPC]_T$ on $k_{obs(u)}$ for Cr(VI) oxidation of glycerol in aqueous $H_2SO_4$ at 30°C. $[Cr(VI)]_T = 5 \times 10^{-4}$ mol $dm^{-3}$, $[glycerol]_T = 0.05$ mol $dm^{-3}$, $[H_2SO_4] = 0.5$ mol $dm^{-3}$. (b) Dependence of $[CPC]_T$ on $k_{obs(c)}$ for Cr(VI) oxidation of glycerol in aqueous $H_2SO_4$ at 30°C. $[Cr(VI)]_T = 5 \times 10^{-4}$ mol $dm^{-3}$, $[glycerol]_T = 0.05$ mol $dm^{-3}$, $[H_2SO_4] = 0.5$ mol $dm^{-3}$, $[PA]_T = 0.075$ mol $dm^{-3}$.

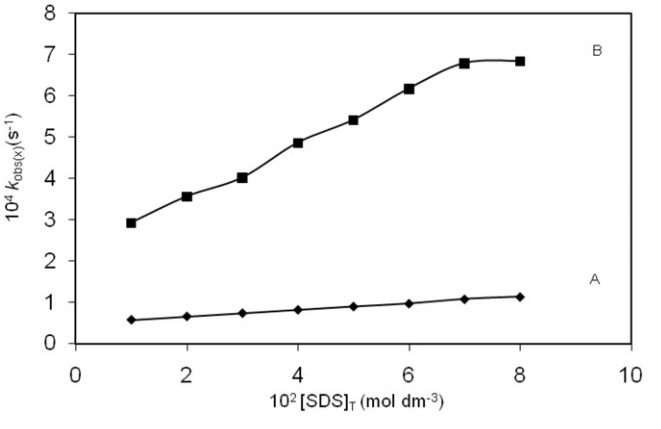


Figure 7. Dependence of $[SDS]_T$ on $k_{obs(x)}$ (where $x$ = u or T) for Cr(VI) oxidation of glycerol in aqueous $H_2SO_4$ at 30°C. $[Cr(VI)]_T = 5 \times 10^{-4}$ mol $dm^{-3}$, $[glycerol]_T = 0.01$ mol $dm^{-3}$, $[H_2SO_4] = 0.5$ mol $dm^{-3}$. $k_{obs(u)}$ for A (in absence of PA) and $k_{obs(T)}$ for B (in presence of PA), where $[PA]_T = 0.01$ mol $dm^{-3}$.

complex (equation (17)) in the aqueous phase, and thus the accumulated neutral substrate in the micellar phase cannot participate in the reaction; consequently, the reaction rate is retarded. Thus in both the uncatalyzed and PA-catalyzed path the reaction is mainly restricted to the aqueous phase, where the reactant concentrations decrease due to their favorable partitioning in the micellar phase.

To intercept the observed kinetic data, the applicability of the pseudo-phase kinetic model proposed by Menger and Portnoy [9] may be considered. This model considers the partitioning of one reactant between the aqueous and micellar phase and leads to rate equation (22),

$$k_{obs} = (k_w + k_m K_B[D_n])/(1 + K_B[D_n]) \tag{22}$$

where $k_w$ and $k_m$ are first-order rate constants in the aqueous and micellar phases, respectively, and include the concentration of the other reactant in these pseudo phases. $K_B$ gives the measure of the binding constant of the reactant (which is partitioned) with the micelles. $[D_n]$ is the concentration of the micelles and is related to the stoichiometric concentration of the surfactant ($[D]_T$), critical micellar concentration (cmc) and the aggregation number ($N$), i.e., $[D_n] = ([D]_T - \text{cmc})/N$. Equation (22) leads to

$$1/(k_w - k_{obs}) = 1/(k_w - k_m) + (N/K_B)\{1/([D]_T - \text{cmc})\}\{1/(k_w - k_m)\} \tag{23}$$

and

$$(k_w - k_{obs})/(k_{obs} - k_m) = P = (K_B/N)[D]_T - (K_B/N)(\text{cmc}) \tag{24}$$

Equations (23) and (24) require the cmc value which is not available exactly under the present kinetic conditions. However, by taking the literature value [38] of cmc ($=10.9 \times 10^{-4}$ mol dm$^{-3}$) under comparable conditions at 30°C, the plot of $1/(k_w - k_{obs})$ *versus* $1/([D]_T - \text{cmc})$ (figure 8) is linear at a fixed concentration of the other reactants. This leads to $k_m \approx 0$ for both $k_{obs(u)}$ and $k_{obs(c)}$. Taking $k_m \approx 0$, equation (22) takes the form

$$1/k_{obs} = 1/k_w + (K_B/N)\{([D]_T - \text{cmc})/k_w\} \tag{25}$$

The linearity of the plot of $1/k_{obs}$ *versus* $([D]_T - \text{cmc})$ (figure 9) has been verified, indicating that the reaction occurs predominantly in the aqueous phase. The $k_w$ value obtained from the intercept is comparable with the experimentally observed value. The binding constant parameter (i.e., $K_B/N$) obtained from this plot conforms to the value obtained using equation (23). The magnitude of the binding constant ($K_B/N$) indicates depletion of the reactant concentration in the aqueous phase, causing a lowering of the rate with increasing surfactant concentration. In fact the reaction is strongly acid catalyzed, but $H^+$ ions are not available in the cationic micellar phase produced by CPC owing to electrostatic repulsion. Consequently, the reaction cannot proceed in the micellar phase even when the Cr(VI)-substrate ester (which needs $H^+$ for redox decomposition, cf equation 8) is absorbed in the micellar pseudo-phase.

The rate data in the presence of surfactants were subjected to the Piszkiewicz model [39] analogous to the Hill model applied to enzyme-catalyzed reactions. The Pisziewicz model relates co-operativity between the neutral species and surfactant to aggregate to form the reactive micelles and its contribution to the rate is given by

$$\log[(k_{obs} - k_w)/(k_m - k_{obs})] = \log P = n \log[D]_T - \log K_D \tag{26}$$

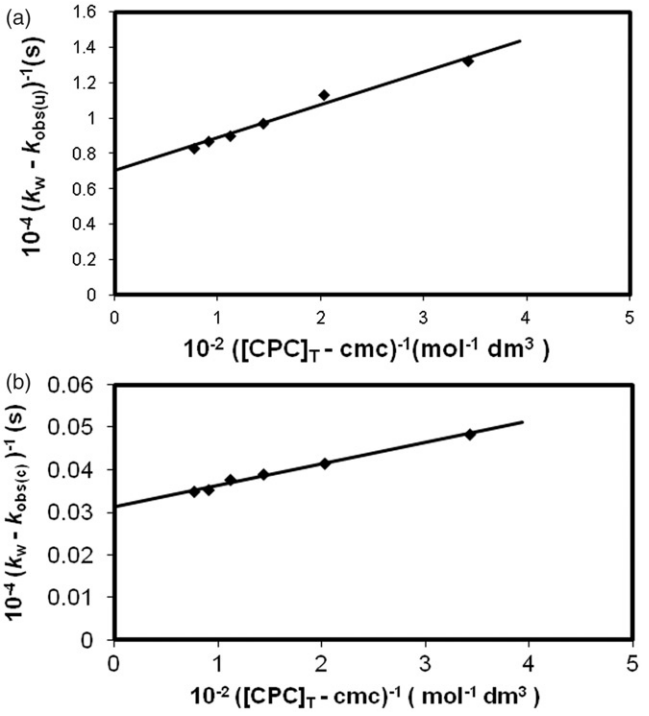


Figure 8. (a) Applicability of the Menger–Portnoy model (i.e., plot of $(k_w - k_{obs(u)})^{-1}$ *vs.* $([CPC]_T - cmc)^{-1}$) to explain the micellar effect on $k_{obs(u)}$ for Cr(VI) oxidation of glycerol in the presence of CPC in aqueous $H_2SO_4$ at 30°C (taking $cmc = 10.9 \times 10^{-4}$ mol dm$^{-3}$) $[Cr(VI)]_T = 5 \times 10^{-4}$ mol dm$^{-3}$, $[glycerol]_T = 0.05$ mol dm$^{-3}$, $[H_2SO_4] = 0.5$ mol dm$^{-3}$. (b) Applicability of the Menger–Portnoy model (i.e., plot of $(k_w - k_{obs(c)})^{-1}$ *vs.* $([CPC]_T - cmc)^{-1}$) to explain the micellar effect on $k_{obs(u)}$ for Cr(VI) oxidation of glycerol in the presence of CPC in aqueous $H_2SO_4$ at 30°C (taking $cmc = 10.9 \times 10^{-4}$ mol dm$^{-3}$) $[Cr(VI)]_T = 5 \times 10^{-4}$ mol dm$^{-3}$, $[glycerol]_T = 0.05$ mol dm$^{-3}$, $[H_2SO_4] = 0.5$ mol dm$^{-3}$, $[PA]_T = 0.075$ mol dm$^{-3}$.



where $K_D$ is the dissociation constant of micellized surfactant back to its components and $n$ is the index of co-operativity. The advantage of equation (26) is that it does not require knowledge of the cmc of the surfactant used. This helps a larger number of data to come under the purview of analysis. Although equation (26) was originally developed for micelle-catalyzed reactions showing a maximum rate followed by inhibition, the model has been applied for different work [34, 35, 40] to explain the miceller effect in which the reaction is inhibited or catalyzed by the micelle over the whole range as observed in the present system. By using equation (26), i.e., the plot of log *P versus* $\log[D]_T$, parameters $n$, $\log[D]_{50}$ (where $\log[D]_{50}$ represents the concentration of surfactant required for half-maximum catalysis or inhibition) and log $K_D$ have been determined (table 2). The calculated $\log[D]_{50}$ values conform well with the experimentally observed values. The values of $n = 1$–2, far less than the aggregation number (20–100) of the surfactant molecules [40] leading to micelles, indicate the existence of catalytically productive submicellar aggregates. The non-integral values of $n$ indicate the existence of multiple equilibria in the formation of catalytically active submicellar aggregates. When the interaction (measured by $-\log K_D$) is fairly high, it is appropriate

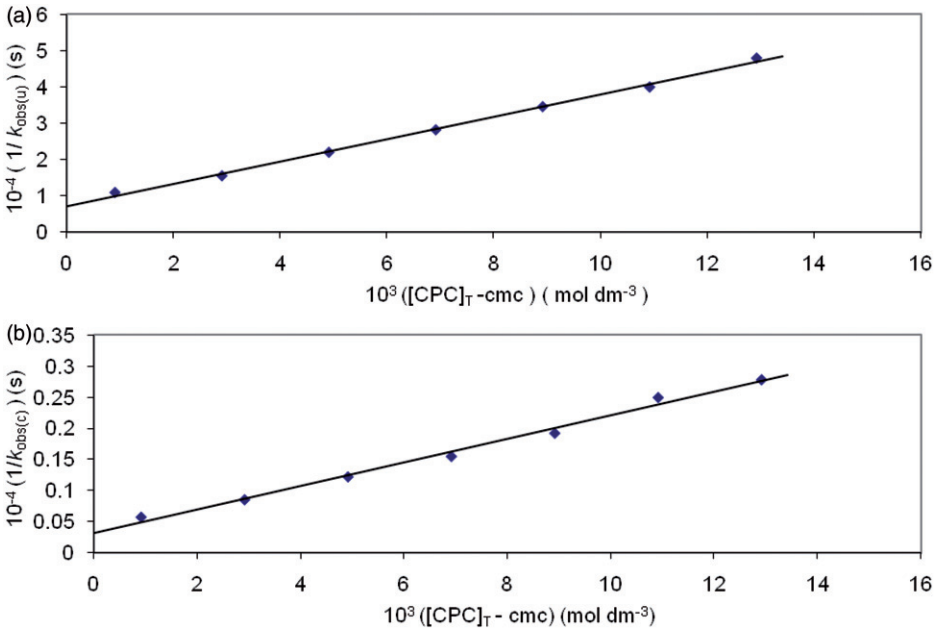


Figure 9. (a) The plot of $1/k_{obs(u)}$ *vs.* ($[CPC]_T - cmc$) to explain the micellar effect on $k_{obs(u)}$ for Cr(VI) oxidation of glycerol in the presence of CPC in aqueous $H_2SO_4$ at 30°C (taking cmc $= 10.9 \times 10^{-4}$ mol dm$^{-3}$) $[Cr(VI)]_T = 5 \times 10^{-4}$ mol dm$^{-3}$, $[glycerol]_T = 0.05$ mol dm$^{-3}$, $[H_2SO_4] = 0.5$ mol dm$^{-3}$. (b) The plot of $1/k_{obs(u)}$ *vs.* ($[CPC]_T - cmc$) to explain the micellar effect on $k_{obs(u)}$ for Cr(VI) oxidation of glycerol in the presence of CPC in aqueous $H_2SO_4$ at 30°C (taking cmc $= 10.9 \times 10^{-4}$ mol dm$^{-3}$) $[Cr(VI)]_T = 5 \times 10^{-4}$ mol dm$^{-3}$, $[glycerol]_T = 0.05$ mol dm$^{-3}$, $[H_2SO_4] = 0.5$ mol dm$^{-3}$, $[PA]_T = 0.075$ mol dm$^{-3}$.

Table 2. Miceller effect on kinetic parameters (30°C) for Cr(VI) oxidation of glycerol in presence and absence of PA.

| | Effect of CPC | | Effect of SDS | |
|---|---|---|---|---|
| Parameters | PA absent[a] | PA present[b] | PA absent[g] | PA present[h] |
| $\log(K_B/N)$ | 2.60[c] | 2.79 | | |
| | 2.63[d] | 2.78 | | |
| | 2.62[e] | 2.76 | | |
| $-\log K_D$ | 2.67[f] | 2.96 | 2.79 | 2.35 |
| $n$ | 1.05 | 1.12 | 1.85 | 1.4 |
| $-\log[D]_{50}$ (calculated) | 2.54 | 2.64 | 1.50 | 1.67 |
| $-\log[D]_{50}$ (found) | 2.50 | 2.60 | 1.45 | 1.69 |

[a]In the absence of PA, i.e., $k_{obs(u)}$: $[Cr(VI)]_T = 5 \times 10^{-4}$ mol dm$^{-3}$, $[S]_T = 0.05$ mol dm$^{-3}$, $[H_2SO_4] = 0.5$ mol dm$^{-3}$.
[b]For PA-catalyzed path, i.e., $k_{obs(c)}$: $[Cr(VI)]_T = 5 \times 10^{-4}$ mol dm$^{-3}$, $[S]_T = 0.05$ mol dm$^{-3}$, $[H_2SO_4] = 0.5$ mol dm$^{-3}$, $[PA] = 0.075$ mol dm$^{-3}$.
[c]Using equation (23).
[d]Using equation (24).
[e]Using equation (25).
[f]Using equation (26).
[g]In the absence of PA, i.e., $k_{obs(u)}$: $[Cr(VI)]_T = 5 \times 10^{-4}$ mol dm$^{-3}$, $[S]_T = 0.01$ mol dm$^{-3}$, $[H_2SO_4] = 0.5$ mol dm$^{-3}$.
[h]For PA-catalyzed path, i.e., $k_{obs(c)}$: $[Cr(VI)]_T = 5 \times 10^{-4}$ mol dm$^{-3}$, $[S]_T = 0.01$ mol dm$^{-3}$, $[H_2SO_4] = 0.5$ mol dm$^{-3}$, $[PA] = 0.01$ mol dm$^{-3}$.

to consider $n$ as representing the average stoichiometry of the detergent–reactant aggregates. The simultaneous applicability of the different kinetic models (i.e., Menger–Portnoy model [9] and Piszkiewicz model [39]) based on different mathematical assumptions is not surprising. In fact, both of these models lead to similar final equations (24) and (26).

**3.8.2. Effect of SDS.** With SDS, a representative anionic surfactant that catalyzes both the uncatalyzed and PA-catalyzed paths, the rate acceleration arises from preferential partitioning of the positively charged Cr(VI)–PA complex (by electrostatic attraction) and neutral substrates in the micellar surface. Thus, SDS allows the reaction to proceed in both the aqueous and micellar interphase. In the absence of PA, binding of $H_2CrO_4$ (kinetically active species [36]) and substrate to the SDS micelles has been suggested by different workers [37]. However, simultaneous partitioning of the neutral Cr(VI)-substrate ester (equation (7)) into the micellar phase cannot be ruled out. However, simultaneous partitioning of $H_2CrO_4$ and substrate is equivalent to partitioning of Cr(VI)-substrate ester. Hence, it leads to higher local concentrations of both reactants at the micelle–water interphase compared with their stoichiometric concentrations. The $H^+$ ions needed for the reaction are also preferably attached to the micellar phase. Thus, SDS allows the reaction in both phases with a preferential rate enhancement in the micellar phase. The observed catalysis can be explained by considering the PIE model [41], which considers the micellar and aqueous phase as two distinct phases, and in the present system the title redox reaction occurs in both phases. The reaction is acid catalyzed and the corresponding exchange equilibrium between $H^+$ and $Na^+$ at the micellar surface is given as

$$H^+_W + Na^+_M \rightleftharpoons H^+_M + Na^+_W \tag{27}$$

The ion-exchange equilibrium constant ($K^H_{ex}$) is defined as

$$K^H_{ex} = [H^+_M][Na^+_W]/[H^+_W][Na^+_M] \tag{28}$$

(Here, the subscripts M and W denote the micellar phase and aqueous phase, respectively).

The concentrations are expressed in terms of the total solution volume and it is further assumed that the activity coefficient ratios $\gamma_M(Na^+)/\gamma_M(H^+)$ and $\gamma_W(Na^+)/\gamma_W(H^+)$ are both equal to unity. Considering the competition only between $Na^+$ and $H^+$, the overall micellar binding parameter is given by (29).

$$\beta = m_H + m_{Na} = [H^+_M]/[D_n] + [Na^+_M]/]D_n] = [H^+_M] + [Na^+_M])/[D_n] \tag{29}$$

Thus, $\beta$ gives the fraction of micellar head groups neutralized. Here $[D_n]$ gives the micellized surfactant concentration, i.e., $[D_n] = [SDS]_T$ – cmc. The various concentration terms are expressed as

$$[H^+_M] = m_H[D_n]$$
$$[H^+_W] = [H^+]_T - [H^+_M] = [H^+]_T - m_H[D_n]$$
$$[Na^+_W] = [Na^+]_T - [Na^+_M] = [Na^+]_T - (\beta - m_H)[D_n]$$
$$[Na^+_M] = [Na^+]_T - [Na^+_W] = (\beta - m_H)[D_n]$$

The ion exchange equilibrium can be expressed as

$$K_{ex}^{H} = m_H\{[Na^+]_T - (\beta - m_H)[D_n]\}/(\beta - m_H)([H^+]_T - m_H[D_n]) \quad (30)$$

On rearrangement equation (30) yields

$$(m_H)^2(K_{ex}^H - 1)[D_n] - m_H\{K_{ex}^H[H^+]_T + [Na^+]_T + \beta[D_n](K_{ex}^H - 1)\} + K_{ex}^H\beta[H^+]_T = 0 \quad (31)$$

Thus $[H_M^+]$ ($=m_H[D_n]$) can be calculated using equation (31). The positively charged Cr(VI)–PA complex (**4** in scheme 2) is the active oxidant ($Ox^+$) in the PA-catalyzed path and it may also participate in a similar exchange equilibrium (32).

$$Ox_W^+ + Na_M^+ \rightleftharpoons Ox_M^+ + Na_W^+ \quad (32)$$

The magnitude of $[Ox_M^+]$ can also be calculated by using the analogous equation (31) involving $K_{ex}^{Ox}$, as in the case of $[H_M^+]$ (equation (28)). For $H^+$ ions, $K_{ex}^H$ is close to unity [37b, 42]. This indicates that there is no specific interaction of $H^+$ or $Na^+$ with the micellar surface and consequently these ions are statistically distributed between the aqueous and micellar phase, if $K_{ex}^H \to 1$, then equation (31) leads to (33).

$$[H_M^+] = ([H^+]_T\beta[D_n])/([H^+]_T + [Na^+]_T) \quad (33)$$

The value of $\beta$ was in the range 0.6–0.85 from conductivity measurements [37b, 42]. It is evident that $[H_M^+]$ increases with increase in $[D_n]$. Similarly, it is reasonable to assume that $[Ox_M^+]$ increases with increase in $[D_n]$ or $[D]_T$. The change in polarity of the medium (specifically in the inter-micellar zone in which the reactants are positioned) with the addition of surfactant may also influence the observed micellar effect [37b]. From the plot of $k_{obs}$ *versus* $[SDS]_T$ (figure 7), it is evident that the rate initially increases but tends to level off at higher $[SDS]_T$. In fact, an increase in $[SDS]_T$ increases the micellar solubilization of the reactant but at the same time an increase in $[SDS]_T$ increases the micellar counter-ion (i.e., $Na^+$), which may displace $H^+$ and $Ox^+$ from the micellar surface to drive the equilibria (27) and (32) to the left. This reduces $[H_M^+]$ and $[Ox_M^+]$ to inhibit the rate process in the micellar phase. Owing to these opposing factors (i.e., dilution of all reactants over micelles at higher $[SDS]_T$), $k_{obs}$ initially increases with increase in $[SDS]_T$, but attains a limiting value at higher $[SDS]_T$. The above micellar effect on $k_{obs}$ has been explained by applying the Piszkiewicz model (plot of logP *vs.* $\log[SDS]_T$), and the values of $n$, $-\log K_D$, $-\log[D]_{50}$ have been evaluated and are given in table 2.

## 4. Conclusion

Oxidations of glycerol by Cr(VI) in the presence of PA (promoter) in aqueous micellar media have been investigated under the condition $[glycerol]_T \gg [Cr(VI)]_T$. Under the kinetic conditions, monomeric Cr(VI) has been found to be kinetically active. Cr(VI)-substrate ester experiences a redox decomposition through 2e transfer at the rate-determining step. The reaction shows both first-order dependence on $[glycerol]_T$ and $[Cr(VI)]_T$, and second-order dependence on $[H^+]$. In the presence of some non-

functional surfactants, the orders remain unchanged. CPC retards the rate, while SDS shows rate acceleration. SDS can be used as catalyst for the production of glyceraldehydes from glycerol. In addition, glycerol can be used to reduce carcinogenic hexavalent chromium to nontoxic trivalent chromium. SDS and PA accelerate the reaction.

## Acknowledgments

We thank CSIR, New Delhi, for financial support.



## References

[1] (a) N. Deb, S. Bagchi, A.K. Mukherjee. *Mol. Phys*., **108**, 1505 (2010); (b) A.V. Nevidimov, V.F. Razumov. *Mol. Phys*., **107**, 2169 (2009); (c) A.A.P. Khan, A. Mohd, S. Bano, K.S. Siddiqi. *J. Dispersion Sci. Technol*., **32**, 717 (2011); (d) S.K. Ghosh, A. Basu, K.K. Paul, B. Saha. *Mol. Phys*., **107**, 615 (2009); (e) N. Kumaraguru, K. Santhakumar. *J. Coord. Chem*., **62**, 3500 (2009); (f) M.A. Malik, F. Nabi, Z. Khan. *J. Dispersion Sci. Technol*., **29**, 1396 (2008); (g) M.A. Malik, R.A. Sheikh, S.A. Al-Thabaili, A.Y. Obaid, Z. Khan. *J. Dispersion Sci. Technol*., **32**, 1173 (2011); (h) N. Ahmed, M.A. Malik, S.A. Al-Thabaili, A.Y. Obaid, Z. Khan. *J. Dispersion Sci. Technol*., **32**, 35 (2010); (i) Y.R. Katre, K. Sahu, S. Patil, A.K. Singh. *J. Dispersion Sci. Technol*., **30**, 481 (2009); (j) R. Saha, A. Ghosh, B. Saha. *J. Coord. Chem*., **64**, 3729 (2011).

[2] (a) T. Dwars, E. Paetzold, G. Oehme. *Angew. Chem. Int. Ed*., **44**, 7174 (2005); (b) S.H. Seo, J.Y. Chang, G.N. Tew. *Angew. Chem. Int. Ed*., **45**, 7526 (2006); (c) J.Y. Ryu, D.J. Hong, M. Lee. *Chem. Commun*., 1043 (2008).

[3] A.K. Das. *Coord. Chem. Rev*., **248**, 81 (2004).

[4] (a) J.F. Scamehorn, J.H. Harwell. *Surfactant-Based Separation Process*, Vol. 33, Surfactants Science Series, Marcel Dekker, New York (1989); (b) H.U. Hebbar, A.B. Hemavathi, B. Sumana, K.S.M.S. Raghavarao. *Sep. Sci. Technol*., **46**, 1656 (2011); (c) X. Zhou, T. Jin, L. Dong, S. Zheng, J. Xiao. *Sep. Sci. Technol*., **44**, 3632 (2009).

[5] (a) J.H. Fandler, E.J. Fendler. *Catalysis in Miceller and Macromolecular Systems*, Academic Press, New York (1975); (b) W. Gan, C. Fellay, P.J. Dyson, G. Laurenczy. *J. Coord. Chem*., **63**, 2685 (2010).

[6] (a) J.F. Rathman. *Curr. Opin. Colloid Interface Sci*., **1**, 514 (1996); (b) P. Alexandris, T.A. Hatton. *Colloid Surf*., **1**, 96 (1995); (c) P.V. Coveney, J.A.D. Wattis. *Mol. Phys*., **104**, 177 (2006); (d) S.-P. Ju, M.-L. Liao, S.-H. Yang, W.-J. Lee. *Mol. Phys*., **105**, 429 (2007).

[7] C. Minero, E. Pramauro, E. Pelizzetti, D. Meisel. *J. Phys. Chem*., **87**, 399 (1983).

[8] M.N. Khan. *J. Colloid Interface Sci*., **170**, 598 (1995).

[9] F.M. Menger, C.E. Portnoy. *J. Am. Chem. Soc*., **89**, 4689 (1967).

[10] C.A. Bunton. *Catal. Rev. Sci. Eng*., **20**, 1 (1979).

[11] (a) R. Saha, R. Nandi, B. Saha. *J. Coord. Chem*., **64**, 1782 (2011); (b) B. Saha, C. Orvig. *Coord. Chem. Rev*., **254**, 2959 (2010).

[12] M. Islam, B. Saha, A.K. Das. *J. Mol. Catal. A: Chem*., **236**, 260 (2005).

[13] R. Bayen, M. Islam, A.K. Das. *Carbohydr. Res*., **340**, 2163 (2005).

[14] (a) M. Islam, B. Saha, A.K. Das. *Int. J. Chem. Kinet*., **38**, 531 (2006); (b) K.M. Chowdhuri, J. Mandal, B. Saha. *J. Coord. Chem*., **62**, 1871 (2009); (c) J. Mandal, K.M. Chowdhuri, K.K. Pal, B. Saha. *J. Coord. Chem*., **63**, 99 (2010).

[15] M. Islam, A.K. Das. *Carbohydr. Res*., **343**, 2308 (2008).

[16] M. Islam, A.K. Das. *Prog. React. Kinet. Mech*., **33**, 219 (2008).

[17] S. Smith, P. Althouse, J. Shigley. *J. Org. Chem*., **25**, 303 (1960).

[18] A.I. Vogel. *Elementary Practical Organic Chemistry, Part III, Quantitative Organic Analysis*, p. 739, ELBS and Longman Group Ltd., London (1958).

[19] V. Daier, S. Signoirella, M. Rizzotto, M.I. Frascaroli, C. Palopali, C. Brondino, J.M. Salas-Peregrin, L.F. Sala. *Can. J. Chem*., **77**, 57 (1999).

[20] (a) B.N. Figgis. *Introduction to Ligand Fields*, p. 222, Wiley Eastern Limited, New Delhi, India (1966); (b) C.K. Jorgensen. *Absorption Spectra and Chemical Bonding in Complexes*, p. 290, Pergamon Press Ltd., Oxford/London (1964).

[21] (a) T.Y. Lin, H.W. Zeng, C.M. Chuo. *J. Chin. Chem. Soc.*, **42**, 43 (1995); (b) Z. Khan, Kabir-ud-Din. *Transition Met. Chem.*, **27**, 832 (2002).
[22] J. Rocek, F.H. Westheimer. *J. Am. Chem. Soc.*, **84**, 2241 (1962).
[23] A. Basu, S.K. Ghosh, T. Ghosh, R. Saha, R. Nandi, B. Saha. *Tenside Surfac. Detergent*, **48**, 453 (2011).
[24] V.M.S. Ramanujan, N. Venkatasubramaniam, S. Sundaram. *Aust. J. Chem.*, **30**, 325 (1977).
[25] (a) F. Hasan, J. Rocek. *Tetrahedron*, **30**, 21 (1974); (b) J. Rocek. *Collect. Czech. Chem. Commun.*, **25**, 1052 (1960); (c) M. Rahman, J. Rocek. *J. Am. Chem. Soc.*, **93**, 5455 (1971).
[26] (a) J.F. Perez-Benito, C. Arias, D. Lamrahri. *J. Chem. Soc., Chem. Commun.*, 427 (1992); (b) J.F. Perez-Benito, C. Arias. *Can. J. Chem.*, **71**, 649 (1993).
[27] W. Watanable, F.H. Westheimer. *J. Chem. Phys.*, **17**, 61 (1949).
[28] P.R. Bontchev, M. Malinovski, M. Mitewa, K. Kabassonov. *Inorg. Chim. Acta*, **6**, 499 (1972).
[29] F.W. Bilmeyer. *Text Book of Polymer Sciences*, Vol. 85, Wiley, New York (1984).
[30] (a) A.C. Chatterjee, S.K. Mukherjee. *J. Am. Chem. Soc.*, **80**, 3600 (1958); (b) T.J. Kemp, W.A. Waters. *Proc. Roy. Soc.*, **274**, 480 (1965).
[31] (a) J. Rocek, T.Y. Peng. *J. Am. Chem. Soc.*, **99**, 7622 (1977); (b) A.K. Das. *Inorg. React. Mech.*, **1**, 161 (1999); (c) M. Islam, B. Saha, A.K. Das. *J. Mol. Catal A: Chem.*, **266**, 21 (2007); (d) B. Saha, M. Islam, A.K. Das. *Inorg. React. Mech.*, **6**, 141 (2006); (e) B. Saha, M. Das, R.K. Mohanty, A.K. Das. *J. Chin. Chem. Soc.*, **51**, 399 (2004); (f) B. Saha, M. Das, A.K. Das. *J. Chem. Res.*, 658 (2003).
[32] L. Moyne, G. Thomas. *Anal. Chim. Acta*, **31**, 503 (1964).
[33] C.A. Bunton, G. Cerichelli. *Int. J. Chem. Kinet.*, **12**, 519 (1980).
[34] G.P. Panigrahi, B.P. Sahu. *J. Indian Chem. Soc.*, **68**, 239 (1991).
[35] N.C. Sarada, I.A.K. Reddy. *J. Indian Chem. Soc.*, **70**, 35 (1993).
[36] (a) K.K. Sengupta, T. Samanta, S.N. Basu. *Tetrahedron*, **42**, 681 (1986); (b) E. Rodenas, E. Perez-Benito. *J. Phys. Chem.*, **95**, 9496 (1991).
[37] (a) G.P. Panigrahi, S.K. Mishra. *Indian J. Chem.*, **32A**, 956 (1993); (b) B. Sankararaj, S. Rajagopal, K. Pitchumani. *Indian J. Chem.*, **34A**, 440 (1995).
[38] A. Chatterjee, S.P. Moulik, S.K. Sanyal, B.K. Mishra, P.M. Puri. *J. Phys. Chem. B*, **105**, 12823 (2001).
[39] D. Piszkiewicz. *J. Am. Chem. Soc.*, **98**, 3053 (1977).
[40] (a) Z. Khan, S.I. Ali, Z.A. Rafique, Kabir-ud-Din. *Indian J. Chem.*, **36A**, 579 (1997); (b) D.S. Gour. *J. Indian Chem. Soc.*, **74**, 545 (1997); (c) K.K. Ghosh, S.K. Sar. *J. Indian Chem. Soc.*, **75**, 39 (1998).
[41] C.A. Benton, F. Nome, F.H. Quina, L.S. Romsted. *Acc. Chem. Res.*, **24**, 357 (1991).
[42] E. Perez-Benito, E. Rodenas. *Langmuir*, **7**, 232 (1991).